2018-10-25

Red wine and green tea flavonoids are cis-allosteric activators and competitive inhibitors of GLUT1-mediated sugar uptake

Ogooluwa A. Ojelabi
University of Massachusetts Medical School

Et al.

JBC Papers in Press. Published on October 25, 2018 as Manuscript RA118.002326
The latest version is at http://www.jbc.org/cgi/doi/10.1074/jbc.RA118.002326

Red wine and green tea flavonoids are cis-allosteric activators and competitive inhibitors of GLUT1-mediated sugar uptake

By

Ogooluwa A. Ojelabi, Kenneth P. Lloyd, Julie K. De Zutter and Anthony Carruthers

From the Department of Biochemistry and Molecular Pharmacology, Graduate School of Biomedical Sciences, University of Massachusetts Medical School, Worcester, Massachusetts, 01605

Running title: Flavonoids are exofacial, GLUT1 ligands

Address correspondence to: Anthony Carruthers, PhD., 364 Plantation Street, LRB Room 926 Worcester, MA 01605. Phone: 508-856-5570; Fax: 508-856-6464; E-mail: anthony.carruthers@umassmed.edu

Keywords: glucose transport; structure-function; membrane transport; allosteric regulation, oligomerization

Abstract

The anti-oxidant, flavonoid-rich content of red wine and green tea is reported to offer protection against cancer, cardiovascular disease and diabetes. Some studies, however, show that flavonoids inhibit GLUT1-mediated, facilitative glucose transport raising the possibility that their interaction with GLUT1 and subsequent, downstream effects on carbohydrate metabolism may also impact health. The present study explores the structure/function relationships of flavonoid-GLUT1 interactions. We find that low concentrations of flavonoids act as cis-allosteric activators of sugar uptake while higher concentrations competitively inhibit sugar uptake and non-competitively inhibit sugar exit. Studies with heterologously expressed human GLUTs 1, 3 and 4 reveal that quercetin-GLUT1 and -GLUT4 interactions are stronger than quercetin-GLUT3 interactions, that ECG is more selective for GLUT1 while EGCG is less isoform-selective. Docking studies suggest that only one flavonoid can bind to GLUT1 at any instant, but sugar transport and ligand binding studies indicate that human erythrocyte GLUT1 can bind at least two flavonoid molecules simultaneously. Quercetin and EGCG are each characterized by positive, cooperative binding whereas EGC shows negative cooperative binding. These findings support recent studies suggesting that GLUT1 forms an oligomeric complex of interacting, allosteric, alternating access transporters. We discuss how modulation of facilitative glucose transporters could contribute to the protective actions of the flavonoids against diabetes and Alzheimer's.

Moderate consumption of red wine or green tea is associated with protection against cancer, cardiovascular disease and diabetes (*1–4*). These benefits are hypothesized to result from the flavonoid-rich, antioxidant capacity of the beverages (*5*). The present study investigates an alternative pathway by which the flavonoids may impact organismal health - direct interaction with the facilitative glucose transporters GLUT1, GLUT3 and GLUT4 leading to downstream effects on carbohydrate metabolism.

The flavonoids are a large group of polyphenolic secondary metabolites with over 4,000 types identified in fruits, flowers, vegetables and leaves (*5*, *6*). The general structure of flavonoids is a flavan backbone (Figure 1A) consisting of 2 benzene rings linked together by a heterocyclic pyran ring (*7*). Substitutions in the flavan structure by hydroxyls, methyl groups and sugars create the wide range of flavonoid derivatives (*5*). Quercetin, epigallocatechin gallate (EGCG) and epicatechin gallate (ECG) are present in red wine and green tea and are among the most extensively characterized flavonoids. Each cup of green tea is estimated to contain up to 300 mg EGCG, 49 mg ECG and 14 mg quercetin (*8–10*). Red wine contains 4–16 mg/L quercetin (*11*, *12*) but while EGCG and ECG are known to present in red wine (*8*) their levels are not well defined. The health benefits of the flavonoids have been attributed to their strong anti-oxidant capacity. The flavonoids chelate metal

ions such as Fe^{3+}, and trap reactive species including singlet oxygen, superoxide radicals, nitric oxide, and peroxynitrite (*5*, *13*, *14*).

Some studies, however, show that quercetin, EGCG and ECG inhibit GLUT1-mediated facilitative glucose transport (*15*, *16*) raising the possibility that it is their interaction with GLUT1 and their downstream effects on carbohydrate metabolism that impact health. While this may explain their actions in cancer where GLUT1 expression and non-oxidative glucose metabolism are upregulated (*17*), it is harder to understand how sugar transport inhibition would ameliorate diabetes and cardiovascular disease.

Recent studies have suggested that GLUT1 forms an oligomer complex of interacting, allosteric, alternating access transporters (*18*, *19*) and that low concentrations of GLUT1 inhibitors acting at exofacial or endofacial sugar binding sites stimulate sugar transport (*18*, *20*). The present study explores the detailed structure/function relationships of flavonoid-GLUT1 interactions in order to explicate flavonoid action on cellular function. We find that the flavonoids act as heterotropic, cis-allosteric activators of sugar uptake at low concentrations and as competitive inhibitors of sugar uptake at higher concentrations. While some health benefits of flavonoids may indeed derive from their anti-oxidant capacities, future studies should also consider how the dual actions of flavonoids on glucose transport may influence downstream glucose metabolism in tumors, in insulin-secreting and responsive tissues and in the CNS.

Results

Dietary flavonoids are reported to impair cellular sugar transport to varying degrees in different cell types (*16*, *21–25*). We therefore examined the effects of quercetin, EGCG and ECG (Figures 1B-1D) on GLUT1-mediated, zero-trans uptake of 3-O-methylglucose (3MG, a transported but non-metabolized sugar) in human red blood cells. Quercetin, EGCG and ECG inhibit uptake of 0.1 mM 3MG in a dose-dependent manner, with $K_{i(app)}$ = 1.88 ± 0.33 μM, 9.63 ± 1.95 μM, and 1.90 ± 0.32 μM respectively (Figure 1E).

We determined the sidedness of flavonoid action on GLUT1 by examining their effects on 2 modes of red cell sugar transport: 1) zero-trans 3MG uptake (influx into sugar-free cells), and 2) zero-trans 3MG exit (efflux from sugar-loaded cells into medium lacking sugar). Transport theory informs us (*26*, *27*) that a ligand competing with sugar for binding at the exofacial sugar binding site serves as a competitive inhibitor of sugar uptake and as a noncompetitive inhibitor of sugar exit. Conversely, a ligand competing with sugar for binding at the endofacial sugar binding site serves as a noncompetitive inhibitor of sugar uptake and as a competitive inhibitor of exit.

The effects of the flavonoids on the concentration-dependence of initial rates of 3MG uptake are shown in Figure 2A. Using the Extra Sum of Squares F-test (*28*) to test the null hypothesis that 3MG uptake is described equally well by non-saturable sugar uptake (uptake = k*[S]), by Michaelis-Menten uptake (Equation 2) and by Michaelis-Menten uptake plus non-saturable uptake fails for all conditions. All uptakes are best described by simple Michaelis-Menten kinetics. Analysis of 3MG uptakes by non-linear regression analysis using equation 2 reveals that the flavonoids increase $K_{m(app)}$ for sugar uptake from 2.39 ± 0.36 mM to 11.07 ± 5.03 mM (quercetin), 10.64 ± 2.63 mM (EGCG) and 7.14 ± 2.63 mM (ECG), without significantly affecting V_{max} for uptake (1.202 ± 0.082 mmol/L cell water/min; Figure 2A; Table 1). Lineweaver-Burk analysis results in lower estimates of V_{max} and $K_{m(app)}$ (Figure 2A inset and Table 1) but the same conclusion (V_{max} is unchanged but $K_{m(app)}$ is increased). This suggests that quercetin, EGCG and ECG inhibit GLUT1-mediated sugar uptake by binding at the exofacial 3MG binding site or at a site whose occupancy is mutually exclusive with 3MG occupancy of the exofacial sugar binding site. Consistent with this idea, the flavonoids act as noncompetitive inhibitors of net 3MG exit: they are without effect on $K_{m(app)}$ (12.9 mM) for exit, but decrease V_{max} for exit by more than 2-fold from 2.03 mmol/L cell water/min to 0.89 (quercetin), 0.72 (EGCG), and 0.60 mmol/L cell water/min (ECG; Figure 2B).

We have previously shown that low concentrations of exofacial inhibitors (e.g. WZB117 and maltose) or endofacial inhibitors (e.g cytochalasin B) of GLUT1-mediated sugar transport modestly stimulate red cell sugar uptake (*20*,

29, *30*). Consistent with these reports, quercetin (≤ 0.5 μM), EGCG (≤ 2.5 μM) and ECG (≤ 0.5 μM) reproducibly stimulate erythrocyte zero-trans 3MG uptake by up to 35% ($p < 0.05$; Figure 3). These results suggest that GLUT1 presents at least 2 exofacial flavonoid binding sites – one that stimulates sugar uptake and a second site that inhibits uptake.

CB is a membrane-permeant, GLUT1 inhibitor which binds at or close to the endofacial glucose binding site (*26*, *27*). Extracellular maltose, but not glucose, inhibits equilibrium binding of the CB to the endofacial glucose binding site of GLUT1 (*29*, *31*, *32*). We therefore asked if the flavonoids, which appear to act as exofacial ligands, also interfere with GLUT1 equilibrium [^{3}H]-CB binding. Quercetin, EGCG, ECG, and nonradioactive CB inhibit [^{3}H]-CB binding to GLUT1 with $K_{i(app)}$ (assuming simple inhibition (*33*)) of 0.637 ± 0.071 μM, 6.097 ± 0.726 μM, 0.871 ± 0.103 μM, and 0.055 ± 0.003 μM respectively (Figure 4A). While these curve fits produce good correlation coefficients ($R^2 > 0.91$ in all cases), the standard deviation of the residuals of each fit (≥ 0.09; excluding CB) is greater than 20% of the standard deviation of the y values suggesting that the fits are poor.

Closer examination reveals that inhibition by quercetin and EGCG increases more steeply while inhibition produced by ECG increases less steeply than is expected for simple. Michaelis-Menten inhibition. Inhibition of radiolabeled CB binding by unlabeled CB is well-described by simple, Michaelis-Menten inhibition. We therefore asked if quercetin, EGCG and ECG inhibition of CB binding are better approximated by inhibition involving multiple, cooperative ligand binding sites and applied a simple, Hill-type model (*33*) to analyze these results (Figure 4B). This analysis produces fits with residuals that do not deviate significantly from zero and the standard deviation of the residuals is significantly reduced. The analysis indicates that quercetin, EGCG, ECG and CB interact with Hill Coefficients (n, (*34*)) of 1.49 ± 0.13, 1.41 ± 0.16, 0.75 ± 0.08 and 0.99 ± 0.05 sites per CB binding site respectively with inhibitory constants (K') of 1.02 ± 0.10, 23.75 ± 9.07, 1.24 ± 0.12 and 0.10 ± 0.01 μM respectively. Hill coefficients greater than 1 indicate multiple ligand binding sites interacting with positive cooperativity whereas Hill coefficients significantly less than 1 indicate multiple ligand binding sites (*34*) but could may also indicate multiple sites which interact with negative cooperativity (33,34). Application of the Extra Sum of Squares F-test (*28*) indicates for the range of inhibitor concentrations used, that the Hill-model provides a significantly better fit for quercetin ($p = 0.0002$), EGCG ($p = 0.0033$) and ECG ($p = 0.0084$) data sets than the simple inhibition model but that both models adequately describe inhibition of [^{3}H]-CB binding by unlabeled CB.

To further test the effects of flavonoids on CB binding to erythrocyte GLUT1, we measured the concentration dependence of CB inhibition of 3MG (0.1 mM) uptake ± flavonoids. The presence of quercetin (2 μM), EGCG (20 μM) or ECG (5 μM) inhibits basal sugar uptake (uptake in the absence of CB) and increases $K_{i(app)}$ for CB inhibition of 3MG uptake by at least 2.5-fold (Figure 4C). Assuming simple competition between the flavonoids and CB for binding to GLUT1 (but see Figure 4B), the computed $K_{i(app)}$ for quercetin (2 μM), EGCG (20 μM) and ECG (5 μM) inhibition of CB inhibition ($K_{i(app)}$ = 0.24 ± 0.03 μM) of transport are 1.88 ± 0.33, 9.63 ± 1.95 and 1.90 ± 0.32 μM respectively. These results indicate that exofacial inhibitors impair CB binding to the GLUT1 endofacial sugar binding site and thereby reduce the potency of CB inhibition of sugar transport.

To act as cytoplasmic antioxidants, the flavonoids must cross the cell membrane. Previous studies have suggested that dietary flavonoids enter cells both by protein-independent trans-bilayer diffusion (*35*, *36*), and via carrier proteins, including GLUT1, GLUT4, SGLT1 and MCT (*15*, *37–40*).

Incubation of RBCs with 1 μM [^{3}H]-quercetin at 4ºC for 0.25 to 30 minutes indicates that the flavonoid achieves equilibrium association with RBCs within 30 seconds of exposure to the cells. The [^{3}H]-quercetin equilibrium space of the cells is 70% of the equilibrium [^{3}H]-3MG space of RBCs (Figure 5A). If quercetin enters cells via GLUT1, as suggested by Cunningham et al (*15*), [^{3}H]-quercetin uptake in human erythrocytes should be inhibited by inhibitors of sugar transport. CB (20 μM) almost completely inhibits [^{3}H]-3MG

uptake, but is without effect on [^{3}H]-quercetin association with human RBCs (Figure 5B).

We investigated potential interactions of β-D-glucose, quercetin, EGCG and ECG with the exofacial sugar binding site by molecular docking using the homology modeled GLUT1 outward-open structure (GLUT1-e2; ((*18*)). The exofacial, interstitium-exposed cavity of GLUT1-e2 presents 3 potential β-D-glucose docking sites - peripheral, intermediate and core (*18*, *20*). Benzene ring A (Figure 1A–D) in quercetin, EGCG and ECG overlaps with the proposed core β-D-glucose docking site ((*20*); and Figure 6A–D) while benzene ring B in quercetin interacts with intermediate and peripheral sites via hydrogen bonding and/or hydrophobic interactions (Figure 6B). In EGCG and ECG, benzene ring B is inverted 45º, and makes additional interactions with the core β-D-glucose docking site, while their gallate group overlaps with the intermediate β-D-glucose docking site (Figures 6C & D).

The residues contributing to β-D-glucose docking at core, intermediate, and peripheral β-D-glucose sites have been previously described (*20*). Figures 6E–H illustrate the putative hydrogen bond and hydrophobic contacts of core β-D-glucose, quercetin, EGCG and ECG with GLUT1-e2. All ligands form 5 common hydrophobic interactions (Ile164, Val165, Ile168, Phe291 & Phe379), and 1 hydrogen bond interaction at Glu380 (Figures 6E-H). Additionally, each inhibitor forms hydrogen bonds with Asn34 and Gln283 (Figures 6F–H), but quercetin forms 3 additional hydrogen bonds (Gln283, Glu380 and Asn415; Figure 6F). EGCG and ECG form more hydrophobic contacts with GLUT1-e2 than quercetin (Figure 6G & H).

Neuronal GLUT3, and insulin-sensitive GLUT4 share 93% and 85% sequence similarity with GLUT1 respectively (*41*). We therefore asked if quercetin, EGCG and ECG inhibitions of GLUT3 and GLUT4 resemble their inhibition of GLUT1 or if these inhibitors present an unanticipated selectivity towards these proteins. We transiently expressed hGLUT1, hGLUT3 or hGLUT4 into HEK293 cells and assayed for dose-dependent inhibition of 100 μM 2-deoxy-D-glucose (2DG) uptake at 37 ºC. Our previous studies have shown that heterologous expression of hGLUT1, hGLUT3 or hGLUT4 suppresses expression of endogenous GLUT3 message and protein in HEK293 cells (*20*). All experiments were paired and relative 2DG uptake (v_i/v_c) by HEK293 cells was expressed as a function of [flavonoid]. Over the range of concentrations used, quercetin and EGCG inhibit GLUT1-, GLUT3- and GLUT4-mediated 2DG uptake in HEK-293 cells (Figures 7A–B). ECG has a bimodal effect on 2DG uptake first stimulating then inhibiting transport (Figure 7C). The curves drawn through the hGLUT1 data (dashed lines) were computed using equation 3 and the parameters computed for flavonoid inhibitions of RBC-mediated 3MG transport shown in Fig 3. Notwithstanding the limited dose response range of Figure 7A, the use of a different substrate (2DG vs 3MG) and the elevated assay temperature (37 vs 4ºC) where the flavonoids are susceptible to more rapid decomposition (42), the agreement between flavonoid-inhibitions of heterologously expressed hGLUT1 and RBC-resident hGLUT1 is strong. The curves drawn through the hGLUT3 and hGLUT4 data (solid lines) were computed by nonlinear regression using equation 3. Table 1 summarizes our findings. Quercetin shows higher affinity for GLUT1 and GLUT4 than it does for GLUT3. EGCG displays similar avidity for GLUTs 1, 3 and 4. Relative to quercetin and EGCG, ECG has lower affinity for GLUTs 1, 3 and 4.

Docking of quercetin, EGCG and ECG to exofacial GLUT3 and GLUT4 reveals that these ligands coordinate with equivalent residues when docked to the same GLUT isoform, but differ significantly when their interactions are compared across GLUT1, GLUT3 and GLUT4 (Figure 8).

Discussion

Red wine and green tea flavonoids inhibit the facilitative glucose transporter, GLUT1, by interacting at its exofacial sugar binding site. Quercetin, EGCG and ECG competitively inhibit net sugar uptake by human erythrocytes but are noncompetitive inhibitors of red cell sugar exit. Molecular docking studies using homology modeled GLUT1 reveal that quercetin, EGCG, ECG and D-glucose share overlapping interaction sites in the exofacial ligand binding cavity of GLUT1. While docking studies suggest that only one flavonoid can

bind to GLUT1 at any instant, sugar transport and ligand binding studies indicate that the erythrocyte sugar transporter can bind at least two flavonoid molecules simultaneously.

The sidedness of flavonoid action (exofacial) is compatible with previous reports suggesting that quercetin (*21*, *24*), and EGCG (*16*) act as competitive inhibitors of GLUT1-mediated sugar uptake. Consistent with this conclusion, molecular docking analysis suggests that quercetin, EGCG and ECG share overlapping interaction envelopes in the exofacial ligand binding cavity of GLUT1-e2 including the previously defined core β-D-glucose interaction site ((*20*), Figure 6). Docking analysis also suggests that flavonoid binding is coordinated by the side chains of amino acids which form the previously defined exofacial intermediate and peripheral β-D-glucose interaction sites. The validity of our docking analysis is bolstered by the finding that the coordination of β-D-glucose at the core site in homology modeled GLUT1-e2 involves the same amino acid residues coordinating β-D-glucose binding in the β-D-glucose-human GLUT3-e2 crystal complex (*42*). Core β-D-glucose, quercetin, EGCG and ECG all form hydrophobic interactions with GLUT1 Ile164, Val165, Ile168, Phe291 and Phe379; and form a hydrogen bond with Glu380, suggesting that these residues are integral to ligand binding in the exofacial cavity. The chemical structures of EGCG and ECG are almost identical (the one difference being addition of a hydroxyl group at C3' in EGCG) yet our docking analysis reveals no striking differences in EGCG and ECG coordination to GLUT1-e2. Notwithstanding, EGCG inhibits GLUT1 with 5-fold lower affinity than ECG illustrating the limitations of this docking analysis.

Prior equilibrium ligand binding studies demonstrate that extracellular maltose inhibits CB binding at the GLUT1 endofacial sugar binding site (*27*, *29*). Here we show that exofacial quercetin, EGCG and ECG have the same effect. $K_{i(app)}$ for inhibition of CB binding is 1.6 – 3 fold lower than $K_{i(app)}$ for transport inhibition. This is not explained by competition between inhibitor and transported sugar for binding at the exofacial site because GLUT1 saturation by 0.1 mM 3MG is less than 5% ($K_{m(app)}$ for 3MG = 2.4 mM; see Figure 2A). Closer review of flavonoid inhibition of CB binding indicates that Sy.x (root mean square error) for curve fits to the simple inhibition model are poor. Fitting the data to a Hill model comprising multiple cooperative binding sites ((*33*), equation 5) produces significantly better fits for quercetin, EGCG or ECG but not for CB. Moreover, using the Extra Sum of Squares F-test (*28*) to test the null hypothesis that the simple inhibition and Hill models provide equally good fits of the binding data fails for quercetin, EGCG or ECG. These results suggest that GLUT1 CB binding is affected by at least 2 positively cooperative binding sites each for quercetin and EGCG and two or more (possibly negatively cooperative) binding sites for ECG (*32*, *33*). If multiple, exofacial flavonoid binding sites exist, docking analysis suggests they are unlikely to co-exist within the same GLUT1 molecule. Rather, they must be present in adjacent molecules which interact with each cytochalasin B binding GLUT1 protein.

We also considered that flavonoids compete directly with CB for binding at the endofacial sugar binding site. This would explain their displacement of CB from GLUT1 and would also be consistent with demonstrations of cooperativity between endofacial ligand binding sites present in adjacent GLUT1 subunits of the GLUT1 tetramer (*29*, *30*, *44*, *45*). Molecular docking of CB and quercetin to the endofacial orientation of GLUT1 (GLUT1-e1; (*46*)) supports the hypothesis that CB and quercetin could compete for high affinity binding to GLUT1 (not shown). However, inhibition of transport by a molecule that can bind with equal avidity to both exo- and endofacial sugar binding sites should produce noncompetitive inhibition of both net uptake or net exit (*26*, *27*). Since flavonoid inhibition of net uptake is competitive, this possibility is refuted. If an inhibitor were to bind with significantly lower affinity to the endofacial binding site versus the exofacial site, it would not only increase $K_{m(app)}$ for net sugar uptake but also reduce V_{max} for uptake by > 65% (*26*, *27*) and this is not observed.

The actions of the flavonoids on sugar transport demonstrate an additional form of cooperativity which we term cis-allostery (*18*). Quercetin, EGCG and ECG, like other exofacial GLUT1 inhibitors (e.g WZB117; (*20*) and maltose (*29*)), stimulate GLUT1-mediated

sugar uptake at low inhibitor concentrations then inhibit transport as their concentration is raised. This reinforces the idea that at least 2 flavonoid binding sites modulate GLUT1 function. Two possibilities exist: 1) One of these sites is presented by GLUT1 and the second by a non-GLUT1 but nevertheless GLUT1-interacting protein; 2) The flavonoid binding sites exist on individual GLUT1 molecules whose adjacency in the GLUT1 homotetramer (20, 29, 30) results in cooperative interactions. In both instances, flavonoid binding at the first, high affinity site stimulates sugar uptake by flavonoid-free GLUT1 molecules. As flavonoid concentration is raised, ligand and sugar now compete for binding at the GLUT1 exofacial sugar binding site and transport is inhibited. While the former hypothesis cannot be eliminated by the current study, our previous ligand binding (18, 20, 27, 29-32, 43), hydrodynamic analyses (44, 47), biochemical cross-linking (48), freeze-fracture E.M. (47) and co-immunoprecipitation (49) studies of membrane-resident and purified GLUT1 support the latter hypothesis.

Studies with heterologously expressed GLUT1, GLUT3 and GLUT4 indicate that quercetin inhibits GLUT1 and GLUT4 with comparable avidity but is up to 9-fold less potent against GLUT3. EGCG shows similar inhibitory potency towards GLUT1, GLUT3 and GLUT4. ECG appears to be only a very poor inhibitor of sugar uptake in GLUT1-, GLUT3- or GLUT4-expressing HEK293 cells but this conclusion should be tempered by the ligand's reported instability at 37ºC (42).

GLUT1 inhibition at high flavonoid concentrations could explain the anti-cancer action of flavonoids. Small molecule inhibition of cellular sugar transport results in a cascade of downstream events including down-regulation of glycolytic enzymes, cell cycle arrest, and ultimately, cell death (*49*). GLUT1-stimulation by low concentrations of flavonoids could explain their protective actions against diseases such as diabetes (*50-53*) and neurodegenerative diseases (*54-57*), where enhanced cellular glucose uptake could be ameliorative. However, flavonoids also directly or indirectly modulate other cellular targets including MAP kinase, CDKs, HIF-1α, and vimentin (*14*). While some studies suggest that flavonoids may not readily cross the plasma membrane (*58*), others suggest that flavonoids enter cells via carrier proteins including SGLT1 (*37*, *38*, *59*, *60*), MCTs (*39*), GLUT1 (*15*) and GLUT4 (*40*) or via transbilayer diffusion (*35*, *36*). The current study indicates that, while quercetin may cross the plasma membrane, it does so via a CB-insensitive, GLUT1-independent pathway.

While some health benefits of the flavonoids may derive from their anti-oxidant capacities, the dual actions of flavonoids on glucose transport (interaction with the exofacial sugar binding site and at regulatory sites which modulate sugar transport) present new tools to explore glucose transporter function and downstream glucose metabolism in tumors, in insulin-secreting and responsive tissues and in the CNS.

Experimental Procedures

Reagents

Tritium-labeled 3-O-methylglucose ([^{3}H]-3MG), 2-deoxy-D-glucose ([^{3}H]-2DG) cytochalasin B ([^{3}H]-CB) and quercetin ([^{3}H]-quercetin) were purchased from American Radiolabeled Chemicals (St. Louis, MO). Unlabeled 3MG, CB, quercetin, (-)-epigallocatechin gallate (EGCG), (-)-epicatechin gallate (ECG) and phloretin were purchased from Sigma-Aldrich (St. Louis, MO). Phosphate-buffered saline (PBS) was purchased from Thermo Fisher Scientific (Waltham, MA). WZB117 was purchased from EMD Millipore (Billerica, MA).

Solutions

KCl medium comprised 150 mM KCl, 5 mM HEPES, 0.5 mM EDTA, pH 7.4. Stop solution comprised ice-cold KCl medium plus 50 μM WZB117 and 100 μM phloretin. Sugar uptake/exit medium was made up in KCl medium containing 0 – 20 mM 3MG ± inhibitors and contained [^{3}H]-3MG or [^{3}H]-quercetin as indicated. HEK293 solubilization buffer comprised KCl medium with 1% Triton X-100.

Cells

De-identified whole human blood was purchased from Biological Specialty Corporation (Colmar, PA). HEK293 cells were maintained in Dulbecco's modified Eagle's medium (DMEM) supplemented with 10% fetal bovine

serum, 100 units/mL penicillin, and 100 µg/mL streptomycin in a 37 °C humidified 5% CO_2 incubator.

Heterologous expression of GLUTs

Heterologous expression of hGLUT1, hGLUT3 and hGLUT4 in HEK293 cells was as previously described (*49*, *61*). Both hGLUT1 and hGLUT4 contain a myc-epitope in exofacial loop 1 (*61*), while the 13 C-terminal amino acids in hGLUT3 are replaced by the corresponding residues of hGLUT4 (*49*) to facilitate detection of heterologously expressed transporter.

Red blood cell sugar transport measurements

All human erythrocytes sugar transport experiments were performed at 4 ºC as previously described (*20*, *49*). Red blood cells were isolated from whole blood, and glucose-depleted as described previously (*62*). Sugar transport and ligand binding experiments reported below typically involve addition of 2 to 10 volumes of uptake or ligand binding medium ± inhibitor to 1 volume of a 50% suspension of red cells. Our measurements show that preincubating RBCs with increasing volumes of medium containing the test inhibitor, progressively reduces $K_{i(app)}$ for inhibition of sugar transport or cytochalasin B binding. The explanation (*44*) is that the very high GLUT1 content of RBCs depletes $[inhibitor]_{free}$ as it interacts with GLUT1 resulting in an $[inhibitor]_{free} \leq [inhibitor]_{total}$ at the time of transport or ligand binding assay. The most practical solution to this problem is to pre-incubate RBCs with excess volume of uptake or ligand binding medium lacking sugar or CB but containing the inhibitor at the requisite concentration. We observe that $K_{i(app)}$ for test compound inhibition of sugar transport or CB binding approaches its minimum asymptote when preincubation conditions are 1 volume of RBCs to 50 - 400 volumes of preincubation assay medium (the necessary dilution falls with increasing $[inhibitor]_{total}$). We therefore pre-incubated RBCs with 50-400 volumes of assay medium prior to centrifugation and resuspension in uptake or ligand binding medium to ensure optimal equilibration of inhibitor with GLUT1 before performing transport or ligand binding measurements.

Zero-trans uptake

Zero-trans [^{3}H]-3MG or [^{3}H]-quercetin uptake (uptake into cells lacking intracellular sugar or quercetin) was initiated by adding 10 volumes (100 µL) of uptake medium ± inhibitor to 1 volume (10 µL) of sugar-depleted, 50% hematocrit (Ht) red cells, and sugar uptake allowed to proceed for 30 – 60 seconds at 4 ºC. Uptake was stopped by adding 50 volumes (1 mL) of ice-cold stop solution containing 50 µM WZB117 and 100 µM phloretin. Cells were washed one more time in stop solution, lysed in 3% perchloric acid, and radioactivity assayed for in clarified lysates using liquid scintillation counting. Radioactivity measurements were done in duplicates.

Zero-trans exit

Glucose-depleted, packed RBCs were loaded with 10 mM 3MG by incubating 1 volume of cells with 20 volumes of 20 mM 3MG (containing 1 µCi [^{3}H]-3MG/mL of cold 3MG) for 1 hour at 37 ºC. Immediately following 3MG loading, cells were transferred to 4 ºC and preincubated with or without inhibitors for 10 – 15 min. Cell suspension were spun at 10,000 x g for 1 min, and supernatant discarded. One volume (0.5 mL) of sugar-loaded RBCs were added to 50 volumes of KCl medium ± inhibitor on a shaker with magnetic stirrer. Aliquots (0.5 mL) of the suspension were withdrawn at indicated time intervals, and immediately added to 1 mL ice-cold stop solution. Cells were washed again in stop solution, lysed in 3% perchloric acid and assayed in duplicate for radioactivity.

Hek293 cells sugar uptake

All HEK293 cell sugar uptake measurements were performed at 37 ºC, using 100 µM 2-deoxyglucose (2DG plus [^{3}H]-2DG) as described previously (*49*, *63*).

Equilibrium CB binding

CB binding to human red cells was performed as previously described (*20*, *31*). Briefly, 50 µL of sugar-depleted RBC (50% Ht) ± inhibitors were mixed with 50 µL of ice-cold KCl medium containing 40 nM [^{3}H]-CB and 10 µM cytochalasin D for 15 min at 4 ºC, with constant end-over-end rotation. Total [CB] was obtained from 2 x 10 µL of the cell suspension lysed in 100 µL of 3% perchloric acid, and radioactivity assayed for by liquid scintillation counting. To obtain free [CB], cell sus-

pension was centrifuged at 10,000 x g for 30 s, and 2 x 10 µL of clarified supernatant were assayed for radioactivity. Bound [CB] was calculated as Total [CB] – Free [CB].

Homology modeling

The homology models of the outward-open (e2) conformations of GLUT1 and GLUT4 were generated using the maltose-bound human GLUT3 structure (PDB code: 4ZWC) (*42*). Maltose was removed from the GLUT3 structure and chain A was used as the template for modeled structures. Sequence alignments were generated using ClustalX (*69*). Homology models were built using Modeller-9.9 (*70*) and analyzed using PROCHECK (*71*).

Stochastic docking

The crystal structure of outward-open hGLUT3-e2 (4ZWC) (*42*) was obtained from the protein databank (http://www.rcsb.org/pdb/home/home.do). The structures for β-D-Glucose, quercetin, EGCG and ECG were obtained from Pubchem (https://pubchem.ncbi.nlm.nih.gov). Docking was performed using the Schrodinger software suite. The protein structure was preprocessed with the Protein Preparation Wizard, bond orders were assigned, hydrogens added and the H-bond network was optimized. The system was energy minimized using the OPLS 2005 force field. Ligand structures were prepared with the LigPrep module and the pKa of the ligands was calculated using the Epik module. Molecular docking was performed by the GLIDE module in standard-precision (SP) mode and default values for grid generation. Cavities for docking were calculated using the CastP server (http://sts.bioe.uic.edu/castp/) and the grid was centered on the residues forming the cavity. No restraints were used during the docking.

Data analysis

Linear and nonlinear regression analysis of data sets and statistical tests were performed using GraphPad Prism (Version 7.0a; La Jolla, CA).

Michaelis-Menten inhibition of sugar transport is assumed to be described by:

$$v = v_c - \frac{v_c[I]}{K_{i(app)} + [I]} \quad \text{(equation 1)}$$

where v_c is v measured in the absence of inhibitor I, [I] is the concentration of inhibitor and $K_{i(app)}$ is that [I] producing 50% inhibition of uptake.

Michaelis-Menten transport is assumed to be described by:

$$v = \frac{V_{max}[3MG]}{K_{m(app)} + [3MG]} \quad \text{(equation 2)}$$

where V_{max} is the maximum rate of 3MG transport, [3MG] is the concentration of 3MG and $K_{m(app)}$ is the [3MG] where the rate of uptake is V_{max} /2. Sugar exit was analyzed by nonlinear regression analysis using Mathematica 10.4.1.0 (Wolfram Research) assuming that exit follows Michaelis-Menten kinetics and that the first derivative of the exit progress curve represents d[S]/dt at any given [3MG] (*20*).

Transport stimulation followed by inhibition by inhibitors was approximated first by normalizing all uptake to v_c and then using the following model:

$$\frac{v_i}{v_c} = \frac{Const_1 + [I](Const_2 + [I])}{Const_1 + [I](Const_3 + [I]Const_4)} \quad \text{(equation 3)}$$

where v_c is uptake measured in the absence of inhibitor I, v_i is uptake measured in the pres-

ence of inhibitor, [I] is the concentration of inhibitor and $Const_1$ through $Const_4$ are model dependent (*19*).

Inhibition of [^{3}H]-CB binding to GLUT1 by ligands was analyzed by simple competitive inhibition using the model:

$$\frac{[CB]_b^i}{[CB]_b^c} = \frac{K_{i(app)}\left(K_{CB}+[CB]\right)}{K_{CB}[I]+K_{i(app)}\left(K_{CB}+[CB]\right)} \quad \text{(equation 4)}$$

where $[CB]^i_b$ is bound [CB] measured in the presence of inhibitor I, $[CB]^c_b$ is bound [CB] measured in the absence of inhibitor, $K_{i(app)}$ is the apparent inhibitory constant for inhibition of CB binding by inhibitor, I, and K_{CB} is dissociation constant for CB binding to GLUT1.

CB binding was also analyzed using the Hill equation for inhibition of equilibrium binding in which the transporter is allowed to bind more than one molecule of competing ligand, I

$$\frac{[CB]^i_{b/f}}{[CB]^c_{b/f}} = \frac{K'}{K'+[I]^n} \quad \text{(equation 5)}$$

where $[CB]^i_b$ is bound [CB] measured in the presence of inhibitor I, $[CB]^c_b$ is bound [CB] measured in the absence of inhibitor, K' is $K_{d(app)}$ for I binding to GLUT1 to the power of n where n is the number of inhibitor binding sites. Comparisons of quality of model fits were made using the extra sum of squares F-test (*28*) using GraphPad Prism.

Acknowledgments: This work was supported by NIH grants DK36081 and DK44888. We thank Andrew Simon for reviewing the manuscript.

Conflict of interest: The authors declare that they have no conflicts of interest with the contents of this article.

Author contributions: OAO conducted most of the experiments, analyzed the results and wrote most of the paper. KPL constructed the GLUT1 homology models; JKDeZ performed the heterologous expression and transport studies. AC & OAO conceived the idea for the project, analyzed the results and wrote the paper.

Bibliography

1. Kerry, N. L. and Abbey, M. (1997) Red wine and fractionated phenolic compounds prepared from red wine inhibit low density lipoprotein oxidation in vitro. *Atherosclerosis* **135**, 93-102
2. Del Rio, D., Rodriguez-Mateos, A., Spencer, J. P., Tognolini, M., Borges, G. and Crozier, A. (2013) Dietary (poly)phenolics in human health: structures, bioavailability, and evidence of protective effects against chronic diseases. *Antioxid. Redox Signal* **18**, 1818-1892
3. Hung, C. H., Chan, S. H., Chu, P. M. and Tsai, K. L. (2015) Quercetin is a potent anti-atherosclerotic compound by activation of SIRT1 signaling under oxLDL stimulation. *Mol. Nutr. Food Res.* **59**, 1905-1917
4. Martínez-Pérez, C., Ward, C., Turnbull, A. K., Mullen, P., Cook, G., Meehan, J., Jarman, E. J., Thomson, P. I., Campbell, C. J., McPhail, D., Harrison, D. J. and Langdon, S. P. (2016) Antitumour activity of the novel flavonoid Oncamex in preclinical breast cancer models. *Br. J. Cancer* **114**, 905-916
5. Nijveldt, R. J., van Nood, E., van Hoorn, D. E., Boelens, P. G., van Norren, K. and van Leeuwen, P. A. (2001) Flavonoids: a review of probable mechanisms of action and potential applications. *Am. J. Clin. Nutr.* **74**, 418-425
6. Formica, J. V. and Regelson, W. (1995) Review of the biology of Quercetin and related bioflavonoids. *Food Chem. Toxicol.* **33**, 1061-1080

7. Kühnau, J. (1976) The flavonoids. A class of semi-essential food components: their role in human nutrition. *World Rev. Nutr. Diet* **24**, 117-191
8. Sutherland, B. A., Rahman, R. M. and Appleton, I. (2006) Mechanisms of action of green tea catechins, with a focus on ischemia-induced neurodegeneration. *J. Nutr. Biochem.* **17**, 291-306
9. Singh, B. N., Shankar, S. and Srivastava, R. K. (2011) Green tea catechin, epigallocatechin-3-gallate (EGCG): mechanisms, perspectives and clinical applications. *Biochem. Pharmacol.* **82**, 1807-1821
10. Nishimuro, H., Ohnishi, H., Sato, M., Ohnishi-Kameyama, M., Matsunaga, I., Naito, S., Ippoushi, K., Oike, H., Nagata, T., Akasaka, H., Saitoh, S., Shimamoto, K. and Kobori, M. (2015) Estimated daily intake and seasonal food sources of quercetin in Japan. *Nutrients* **7**, 2345-2358
11. Hertog, M. G., Feskens, E. J., Hollman, P. C., Katan, M. B. and Kromhout, D. (1993) Dietary antioxidant flavonoids and risk of coronary heart disease: the Zutphen Elderly Study. *Lancet* **342**, 1007-1011
12. McDonald, Hughes, Burns, Lean, Matthews and Crozier (1998) Survey of the Free and Conjugated Myricetin and Quercetin Content of Red Wines of Different Geographical Origins. *J Agric Food Chem* **46**, 368-375
13. Kim, H. S., Quon, M. J. and Kim, J. A. (2014) New insights into the mechanisms of polyphenols beyond antioxidant properties; lessons from the green tea polyphenol, epigallocatechin 3-gallate. *Redox Biol.* **2**, 187-195
14. Yang, C. S. and Wang, H. (2016) Cancer Preventive Activities of Tea Catechins. *Molecules* **21**, 1679-1698
15. Cunningham, P., Afzal-Ahmed, I., Naftalin, R. and Jtalmans, W. (2006) Docking studies show that D-glucose and quercetin slide through the transporter GLUT1. *J. Biol. Chem.* **281**, 5797-5803
16. Naftalin, R. J., Afzal, I., Cunningham, P., Halai, M., Ross, C., Salleh, N. and Milligan, S. R. (2003) Interactions of androgens, green tea catechins and the antiandrogen flutamide with the external glucose-binding site of the human erythrocyte glucose transporter GLUT1. *Br. J. Pharmacol.* **140**, 487-499
17. Szablewski, L. (2013) Expression of glucose transporters in cancers. *Biochim. Biophys.Acta* **1835**, 164-169
18. Lloyd, K. P., Ojelabi, O. A., De Zutter, J. K. and Carruthers, A. (2017) Reconciling contradictory findings: Glucose transporter 1 (GLUT1) functions as an oligomer of allosteric, alternating access transporters. *J. Biol. Chem.* **292**, 21035-21046
19. Lloyd, K. P., Ojelabi, O. A., Simon, A. H., De Zutter, J. K. and Carruthers, A. (2017) Kinetic Basis of Cis- and Trans-Allostery in GLUT1-Mediated Sugar Transport. *J. Membr. Biol.* 10.1007/s00232-017
20. Ojelabi, O. A., Lloyd, K. P., Simon, A. H., De Zutter, J. K. and Carruthers, A. (2016) WZB117 inhibits GLUT1-mediated sugar transport by binding reversibly at the exofacial sugar binding site. *J. Biol. Chem.* **291**, 26762-26772
21. Vera, J. C., Reyes, A. M., Velasquez, F. V., Rivas, C. I., Zhang, R. H., Strobel, P., Slebe, J. C., Nunez-Alarcon, J. and Golde, D. W. (2001) Direct inhibition of the hexose transporter GLUT1 by tyrosine kinase inhibitors. *Biochemistry* **40**, 777-90.
22. Cermak, R., Landgraf, S. and Wolffram, S. (2004) Quercetin glucosides inhibit glucose uptake into brush-border-membrane vesicles of porcine jejunum. *Br. J. Nutr.* **91**, 849-855
23. Johnston, K., Sharp, P., Clifford, M. and Morgan, L. (2005) Dietary polyphenols decrease glucose uptake by human intestinal Caco-2 cells. *FEBS Lett.* **579**, 1653-1657
24. Pérez, A., Ojeda, P., Ojeda, L., Salas, M., Rivas, C. I., Vera, J. C. and Reyes, A. M. (2011) Hexose transporter GLUT1 harbors several distinct regulatory binding sites for flavones and tyrphostins. *Biochemistry* **50**, 8834-8845
25. Moreira, L., Araújo, I., Costa, T., Correia-Branco, A., Faria, A., Martel, F. and Keating, E. (2013) Quercetin and epigallocatechin gallate inhibit glucose uptake and metabolism by

breast cancer cells by an estrogen receptor-independent mechanism. *Exp. Cell Res.* **319**, 1784-1795
26. Basketter, D. A. and Widdas, W. F. (1978) Asymmetry of the hexose transfer system in human erythrocytes. Comparison of the effects of cytochalasin B, phloretin and maltose as competitive inhibitors. *J. Physiol.* **278**, 389-401
27. Carruthers, A. and Helgerson, A. (1991) Inhibitions of sugar transport produced by ligands binding at opposite sides of the membrane. Evidence for simultaneous occupation of the carrier by maltose and cytochalasin B. *Biochemistry* **30**, 3907-3915
28. Hamakawa, H., Sakai, H., Takahashi, A., Bando, T. and Date, H. (2013) Multi-frequency forced oscillation technique using impulse oscillations: can it give mechanical information about the lung periphery. *Adv. Exp. Med. Biol.* **765**, 73-79
29. Hamill, S., Cloherty, E. K. and Carruthers, A. (1999) The human erythrocyte sugar transporter presents two sugar import sites. *Biochemistry* **38**, 16974-16983
30. Cloherty, E. K., Levine, K. B. and Carruthers, A. (2001) The red blood cell glucose transporter presents multiple, nucleotide-sensitive sugar exit sites. *Biochemistry* **40**, 15549-15561
31. Helgerson, A. L. and Carruthers, A. (1987) Equilibrium ligand binding to the human erythrocyte sugar transporter. Evidence for two sugar-binding sites per carrier. *J. Biol. Chem.* **262**, 5464-5475
32. Sultzman, L. A. and Carruthers, A. (1999) Stop-flow analysis of cooperative interactions between GLUT1 sugar import and export sites. *Biochemistry* **38**, 6640-6650
33. Segel, I. H. (1975) in *Enzyme Kinetics* ed.) John Wiley & Sons, New York
34. Prinz, H. (2010) Hill coefficients, dose-response curves and allosteric mechanisms. *J. Chem. Biol.* **3**, 37-44
35. Uekusa, Y., Kamihira, M. and Nakayama, T. (2007) Dynamic behavior of tea catechins interacting with lipid membranes as determined by NMR spectroscopy. *J. Agric. Food Chem.* **55**, 9986-9992
36. Sirk, T. W., Brown, E. F., Friedman, M. and Sum, A. K. (2009) Molecular binding of catechins to biomembranes: relationship to biological activity. *J. Agric. Food Chem.* **57**, 6720-6728
37. Walgren, R. A., Lin, J. T., Kinne, R. K. and Walle, T. (2000) Cellular uptake of dietary flavonoid quercetin 4'-beta-glucoside by sodium-dependent glucose transporter SGLT1. *J. Pharmacol. Exp. Ther.* **294**, 837-843
38. Wolffram, S., Blöck, M. and Ader, P. (2002) Quercetin-3-glucoside is transported by the glucose carrier SGLT1 across the brush border membrane of rat small intestine. *J Nutr* **132**, 630-635
39. Vaidyanathan, J. B. and Walle, T. (2003) Cellular uptake and efflux of the tea flavonoid (-)epicatechin-3-gallate in the human intestinal cell line Caco-2. *J. Pharmacol. Exp. Ther.* **307**, 745-752
40. Strobel, P., Allard, C., Perez-Acle, T., Calderon, R., Aldunate, R. and Leighton, F. (2005) Myricetin, quercetin and catechin-gallate inhibit glucose uptake in isolated rat adipocytes. *Biochem. J.* **386**, 471-478
41. Joost, H. G., Bell, G. I., Best, J. D., Birnbaum, M. J., Charron, M. J., Chen, Y. T., Doege, H., James, D. E., Lodish, H. F., Moley, K. H., Moley, J. F., Mueckler, M., Rogers, S., Schurmann, A., Seino, S. and Thorens, B. (2002) Nomenclature of the GLUT/SLC2A family of sugar/polyol transport facilitators. *Am. J. Physiol. Endocrinol. Metab.* **282**, E974-6
42. Na Li, Lynne S. Taylor and Lisa J. Mauer (2011) Degradation Kinetics of Catechins in Green Tea Powder: Effects of Temperature and Relative Humidity. J. Agriculture and Food Chemistry 59, 6082-6090
43. Deng, D., Sun, P., Yan, C., Ke, M., Jiang, X., Xiong, L., Ren, W., Hirata, K., Yamamoto, M., Fan, S. and Yan, N. (2015) Molecular basis of ligand recognition and transport by glucose transporters. Nature 526, 391-396

44. Robichaud, T., Appleyard, A. N., Herbert, R. B., Henderson, P. J. and Carruthers, A. (2011) Determinants of ligand binding affinity and cooperativity at the GLUT1 endofacial site. Biochemistry 50, 3137-3148
45. Zottola, R. J., Cloherty, E. K., Coderre, P. E., Hansen, A., Hebert, D. N. and Carruthers, A. (1995) Glucose transporter function is controlled by transporter oligomeric structure. A single, intramolecular disulfide promotes GLUT1 tetramerization. Biochemistry 34, 9734-9747
46. Deng, D., Xu, C., Sun, P., Wu, J., Yan, C., Hu, M. and Yan, N. (2014) Crystal structure of the human glucose transporter GLUT1. Nature 510, 121-125
47. Graybill, C., van Hoek, A.N., Desai, D., Carruthers, A.M., Carruthers, A. (2006) Ultrastructure of Human Erythrocyte GLUT1 Biochemistry, 45, 8096-8107
48. Hebert, D. N. and Carruthers, A. (1992) Glucose transporter oligomeric structure determines transporter function. Reversible redox-dependent interconversions of tetrameric and dimeric GLUT1. J. Biol. Chem. 267, 23829-23838
49. De Zutter, J. K., Levine, K. B., Deng, D. and Carruthers, A. (2013) Sequence determinants of GLUT1 oligomerization: analysis by homology-scanning mutagenesis. J. Biol. Chem. 288, 20734-20744
50. Liu, Y., Cao, Y., Zhang, W., Bergmeier, S., Qian, Y., Akbar, H., Colvin, R., Ding, J., Tong, L., Wu, S., Hines, J. and Chen, X. (2012) A small-molecule inhibitor of glucose transporter 1 downregulates glycolysis, induces cell-cycle arrest, and inhibits cancer cell growth in vitro and in vivo. Mol. Cancer Ther. 11, 1672-1682
51. Kao, Y. H., Hiipakka, R. A. and Liao, S. (2000) Modulation of obesity by a green tea catechin. Am. J. Clin. Nutr. 72, 1232-1234
52. Tsuneki, H., Ishizuka, M., Terasawa, M., Wu, J. B., Sasaoka, T. and Kimura, I. (2004) Effect of green tea on blood glucose levels and serum proteomic patterns in diabetic (db/db) mice and on glucose metabolism in healthy humans. BMC Pharmacol 4, 18
53. Wu, L. Y., Juan, C. C., Hwang, L. S., Hsu, Y. P., Ho, P. H. and Ho, L. T. (2004) Green tea supplementation ameliorates insulin resistance and increases glucose transporter IV content in a fructose-fed rat model. Eur. J. Nutr. 43, 116-124
54. Choi, Y. T., Jung, C. H., Lee, S. R., Bae, J. H., Baek, W. K., Suh, M. H., Park, J., Park, C. W. and Suh, S. I. (2001) The green tea polyphenol (-)-epigallocatechin gallate attenuates beta-amyloid-induced neurotoxicity in cultured hippocampal neurons. Life Sci. 70, 603-614
55. Choi, J. Y., Park, C. S., Kim, D. J., Cho, M. H., Jin, B. K., Pie, J. E. and Chung, W. G. (2002) Prevention of nitric oxide-mediated 1-methyl-4-phenyl-1,2,3,6-tetrahydropyridineinduced Parkinson's disease in mice by tea phenolic epigallocatechin 3-gallate. Neurotoxicology 23, 367-374
56. Jeon, S. Y., Bae, K., Seong, Y. H. and Song, K. S. (2003) Green tea catechins as a BACE1 (beta-secretase) inhibitor. Bioorg. Med. Chem. Lett. 13, 3905-3908
57. Mandel, S. and Youdim, M. B. (2004) Catechin polyphenols: neurodegeneration and neuroprotection in neurodegenerative diseases. Free Radic. Biol. Med. 37, 304-317
58. Yang, C. S., Sang, S., Lambert, J. D. and Lee, M. J. (2008) Bioavailability issues in studying the health effects of plant polyphenolic compounds. Mol. Nutr. Food Res. 52 Suppl 1, S139-S151
59. Day, A. J., Cañada, F. J., Díaz, J. C., Kroon, P. A., Mclauchlan, R., Faulds, C. B., Plumb, G.W., Morgan, M. R. and Williamson, G. (2000) Dietary flavonoid and isoflavone glycosides are hydrolysed by the lactase site of lactase phlorizin hydrolase. FEBS Lett. 468, 166-170
60. Gee, J. M., DuPont, M. S., Day, A. J., Plumb, G. W., Williamson, G. and Johnson, I. T. (2000) Intestinal transport of quercetin glycosides in rats involves both deglycosylation and interaction with the hexose transport pathway. J. Nutr. 130, 2765-2771
61. Vollers, S. and Carruthers, A. (2012) Sequence Determinants of GLUT1-mediated Accelerated-Exchange Transport - Analysis by Homology-Scanning Mutagenesis. J. Biol. Chem. 287, 42533-42544.

62. Cloherty, E. K., Heard, K. S. and Carruthers, A. (1996) Human erythrocyte sugar transport is incompatible with available carrier models. Biochemistry 35, 10411-10421
63. Levine, K. B., Cloherty, E. K., Hamill, S. and Carruthers, A. (2002) Molecular determinants of sugar transport regulation by ATP. Biochemistry 41, 12629-12638
64. Larkin, M. A., Blackshields, G., Brown, N. P., Chenna, R., McGettigan, P. A., McWilliam, H., Valentin, F., Wallace, I. M., Wilm, A., Lopez, R., Thompson, J. D., Gibson, T. J. and Higgins, D. G. (2007) Clustal W and Clustal X version 2.0. Bioinformatics 23, 2947-2948
65. Eswar, N., Eramian, D., Webb, B., Shen, M. Y. and Sali, A. (2008) Protein structure modeling with MODELLER. Methods Mol. Biol. 426, 145-159
66. Laskowski, R. A., Moss, D. S. and Thornton, J. M. (1993) Main-chain bond lengths and bond angles in protein structures. J. Mol. Biol. 231, 1049-1067

Figure Legends

Figure 1

Chemical structures and dose-dependent inhibition of human erythrocyte zero-trans 3MG (0.1 mM) uptake by quercetin, EGCG and ECG. **A**. The Flavan skeleton for over 4,000 identified flavonoids, including quercetin (**B**), epigallocatechin gallate (EGCG) (**C**), and epicatechin gallate (ECG) (**D**). **E**. Ordinate: 3MG uptake in mmol/L cell water/min; Abscissa: [Inhibitor] in μM. Results are shown for quercetin (●), EGCG (△), and ECG (▲). Each point represents the mean ± SEM of at least 3 duplicate measurements. The curves were computed by nonlinear regression assuming that uptake inhibition is described by equation 1 with the following results: quercetin-treated cells (●): $K_{i(app)}$ = 1.88 ± 0.33 μM, R^2 = 0.92, standard error of regression = 0.01 mmol/L cell water/min; EGCG-treated cells (△): $K_{i(app)}$ = 9.63 ± 1.95 μM, R^2 = 0.87, standard error of regression = 0.01 mmol/L cell water/min; ECG-treated cells (▲): $K_{i(app)}$ = 1.90 ± 0.32 μM, R^2 = 0.93 standard error of regression = 0.01 mmol/L cell water/min

Figure 2

Effects of quercetin on the concentration-dependence of zero-trans 3MG uptake (**A**) and zero-trans 3MG exit (**B**). Results are shown for control cells (○), quercetin-treated cells (●), EGCG-treated cells (△), and ECG-treated cells (▲). Each data point represents the mean ± SEM of at least 4 experiments measured in duplicate. **A**, Ordinate: 3MG uptake in mmol/L cell water/min; Abscissa: $[3MG]_o$ in mM. Curves were computed by nonlinear regression assuming uptake is described by equation 2. The results are summarized in Table 1. Inset shows a Lineweaver-Burk transformation of the data. The lines were computed by linear regression and the results are also summarized in Table 1. **B**, Ordinate: $[3MG]_i$ in mmol/L cell water; Abscissa: Time in minutes. Curves were computed by numerical integration and nonlinear regression assuming Michaelis-Menten exit kinetics (equation 2) with the following results: Control cells (○): V_{max} = 2.03 mmol/L cell water/min, $K_{m(app)}$ = 12.9 mM, normalized root mean square error (NRMSE) = 0.011; quercetin (2.5 μM) treatment (●): V_{max} = 0.89 mmol/L cell water/min, $K_{m(app)}$ = 12.7 mM, NRMSE = 0.022; EGCG (1 μM) treatment (△): V_{max} = 0.71 mmol/L cell water/min, $K_{m(app)}$ = 12.30 mM, NRMSE = 0.024; ECG (0.25 μM) treatment (▲): V_{max} = 0.44 mmol/L cell water/min, $K_{m(app)}$ = 13.5 mM, NRMSE = 0.044.

Figure 3

Sub-saturating concentrations of quercetin, EGCG, and ECG stimulate 3MG uptake. Ordinate: Relative 3MG uptake. Abscissa: Concentration of inhibitors in M (log scale). Results are shown for cells treated with quercetin (●), EGCG (△), and ECG (▲). Each data point represents the mean ± SEM of at least 3 duplicate measurements. The curves were computed by nonlinear regression using equation 3 and the parameters producing the best fits are summarized in Table 2.

The following summarizes the quality of the fits: quercetin treatment (●):R^2 = 0.966, standard error of regression (Sy.X) = 0.097; EGCG treatment (△): R^2 = 0.923, sSy.X = 0.128; ECG treatment (▲): R^2 = 0.866, Sy.X = 0.158.

Figure 4

Flavonoids inhibit CB binding to human RBCs. **A**. Inhibition of [^{3}H]-CB binding to human RBCs. Ordinate: Normalized ratio of bound [^{3}H]-CB to free [^{3}H]-CB. Abscissa: [inhibitor],μM (log scale). Results are shown for cells treated with quercetin (●), EGCG (△), ECG (▲) and non-radioactive CB (○). Each data point represents the mean ± SEM of 3 separate duplicate experiments. Curves were computed by nonlinear regression using equation 4 assuming [[^{3}H]-CB] = 0.05 μM and K_{CB} = 0.055 μM, with the following results: quercetin treatment (●): $K_{i(app)}$ = 0.55 ± 0.06 μM, R^2 = 0.948, standard error of regression (Sy.x) = 0.087; EGCG treatment (△): $K_{i(app)}$ = 5.25 ± 0.63 μM, R^2 = 0.949, Sy.x = 0.089; ECG treatment (▲): $K_{i(app)}$ = 0.75 ± 0.09 μM, R^2 = 0.910, Sy.x = 0.094; nonradioactive CB treatment (○): $K_{i(app)}$ = 0.055 ± 0.003 μM, R^2 = 0.988, Sy.x = 0.036. The residuals of the quercetin, EGCG and ECG fits are plotted beneath the inhibition plot. **B.** Reanalysis of the same data set assuming multiple binding sites for competing ligand using the Hill-equation (equation 5). The results are: quercetin treatment (●): $K_{i(app)}$ = 1.02 ± 0.09 μM, n = 1.49 ± 0.13, R^2 = 0.97, Sy.x = 0.064; EGCG treatment (△): $K_{i(app)}$ = 23.75 ± 9.07 μM, n = 1.41 ± 0.16, R^2 = 0.97, Sy.x = 0.074; ECG treatment (▲): $K_{i(app)}$ = 1.24 ± 0.12 μM, n = 0.75 ± 0.08, R^2 = 0.94, Sy.x = 0.082; nonradioactive CB treatment (○): $K_{i(app)}$ = 0.10 ± 0.01 μM, n = 0.99 ± 0.05, R^2 = 0.99, Sy.x = 0.036. The residuals of the quercetin, EGCG and ECG fits are plotted beneath the inhibition plot. **C**. Ordinate: 3MG uptake in mmol/L cell water/min. Abscissa: Concentration of inhibitors in μM (log scale). Results are shown for CB-treated cells (○), and CB-treated cells plus 2 μM quercetin (●), 20 μM EGCG (△) or 5 μM ECG (▲). Each data point represents the mean ± SEM of at least 3 duplicate measurements. Curves were computed by nonlinear regression using equation 1 and have the following results: CB treatment (○): $K_{i(app)}$ = 0.24 ± 0.03 μM, R^2 = 0.94, Sy.x = 0.007; CB + 2 μM quercetin (●): $K_{i(app)}$ = 0.62 ± 0.17 μM, R^2 = 0.83, Sy.x = 0.004; CB + 20 μM EGCG (△): $K_{i(app)}$ = 0.619± 0.123 μM, R^2 = 0.897, Sy.x = 0.004; CB + 5 μM ECG (▲): $K_{i(app)}$ = 0.71 ± 0.12 μM, R^2 = 0.94, Sy.x = 0.002.

Figure 5

Quercetin uptake by RBCs. **A**. Relative [^{3}H]-3MG and [^{3}H]-quercetin spaces of RBCs. Ordinate: Equilibration relative to the equilibrated 3MG space of the cell. Equilibrium [^{3}H]-quercetin (1 μM) uptake is observed within 5 minutes of exposure to cells. [^{3}H]-3MG (100 μM) equilibration is achieved after 30 minutes exposure. Each bar shows the mean ± S.E.M of 3 separate duplicate experiments. Unpaired t test analysis indicates: **, significant difference between the 3MG and quercetin cell volume ($p = 0.0044$). **B.** Effect of CB on [^{3}H]-quercetin and [^{3}H]-3MG uptake by human erythrocytes. Ordinate: Substrate uptake relative to control. Abscissa: Radiolabeled substrate. Results are shown for control (□) and 20 μM CB-treated cells (■). Each bar shows the mean ± S.E.M of 3 separate experiments measured in duplicate. Unpaired t test analysis indicates: ***, significant [^{3}H]-3MG uptake inhibition by CB ($p < 0.0005$), n.s., no significant difference in [^{3}H]-quercetin uptake with or without CB treatment ($p > 0.05$).

Figure 6

Molecular docking of β-D-glucose, quercetin, EGCG and ECG to homology-modeled exofacial GLUT1 conformation. **A**. Homology-modeled exofacial GLUT1 (GLUT1-e2) is shown in cartoon representation, and membrane spanning helixes 1, 3-6, 8-10 are indicated. Ligands – peripheral, intermediate and core β-D-glucose (red, **A, E**); quercetin (cyan, **B, F**); EGCG (sky blue, **C, G**); ECG (light blue, **D, H**) – are shown as spheres complexed with GLUT1-e2. The insets zoom in to illustrate the spatial arrangement of ligand (shown in stick representation) interaction sites

within GLUT1-e2 but with the GLUT1-e2 cartoon eliminated. The boxes (**E – F**) illustrate β-D-glucose (**E),** quercetin **(F),** EGCG **(G)** and ECG **(H)** coordination in the exofacial cavity showing residues that form hydrogen bonds and hydrophobic interactions. The analysis suggests that EGCG & ECG binding to GLUT1-e2 promotes a 45º flip of benzene ring B.

Figure 7

Isoform specificity of sugar transport inhibition by flavonoids. Results are shown for transport inhibition by quercetin (A), EGCG (B) and ECG (C) in transfected HEK293 cells transiently expressing hGLUT1 (●), hGLUT3 (△) or hGLUT4 (▲). Ordinate: relative 2-deoxyglcuose uptake (v_i/v_c); Abscissa: [inhibitor] in M (log scale). The dashed curves are the curves describing quercetin, EGCG and ECG modulations of hGLUT1-mediated 3MG uptake in RBCs at 4ºC (Figure 3) computed using equation 3. The parameters used were those used in Figure 3 with one exception. $Const_4$ for ECG modulation of GLUT1 was reduced 7-fold. The solid curves describe flavonoid modulations of hGLUTs 3 and 4 and were computed by nonlinear regression using equation 3. The parameters describing the best fits are summarized in Table 2. The following summarizes the quality of these fits: quercetin treatment: hGLUT3 (△): $R^2 = 0.998$, Sy.X = 0.017; hGLUT4 (▲): $R^2 = 0.999$, Sy.X = 0.008; EGCG treatment hGLUT3 (△): $R^2 = 0.998$, Sy.X = 0.017; hGLUT4 (▲): $R^2 = 0.999$, Sy.X = 0.008; ECG treatment: hGLUT3 (△): $R^2 = 0.976$, Sy.X = 0.048; hGLUT4 (▲): $R^2 = 0.482$, Sy.X = 0.144. 2DG uptake in untreated, untransfected cells averaged 2.7 ± 0.6 pmol/μg protein/min with a range of 1.6 – 3.8 pmol/μg protein/min. hGLUT1, hGLUT3 and hGLUT4 heterologous expression increased basal 2DG uptake by 6.3 ± 3.3, 3.4 ± 0.8 and 4.5 ± 1.5-fold respectively.

Figure 8

2-dimensional representation of ligands interactions with hm-GLUT1-e2, GLUT3-e2 and hm-GLUT4-e2 interactions Residues within 4Å distance to docking ligand are shown for quercetin (A), EGCG (B) and ECG (C). Residues and contacts are shown in the following color codes: Polar, blue; hydrophobic, green; negatively charged, orange; positively charged, violet; hydrogen bond and its directionality; purple arrow. Pi-stacking, green arrow; solvent exposed regions of ligands are indicated by gray-shaded circles.

[1]Table 1

	V_m (mM/min)	$K_{m(app)}$ (mM)	Sy.X (mM/min)	R^2
[2]Non Linear Regression Analysis using Michaelis Menten equation				
Control	1.20 ± 0.08	2.39 ± 0.36	0.07	0.93
Quercetin	1.98 ± 0.66	11.07 ± 5.03	0.07	0.89
EGCG	2.14 ± 0.39	10.64 ± 2.63	0.05	0.97
ECG	1.72 ± 0.29	7.14 ± 1.85	0.07	0.94
[3]Lineweaver Burk Analysis				
Control	0.95 ± 0.10	1.49 ± 0.24	0.06	1.00
Quercetin	0.68 ± 0.13	2.50 ± 0.04	0.46	0.99
EGCG	1.49 ± 0.17	3.59 ± 0.06	0.32	1.00
ECG	0.83 ± 0.13	2.51 ± 0.04	0.21	1.00

[1]The data of Figure 2a were analyzed by [2]nonlinear regression analysis assuming Michaelis-Menten kinetics (equation 2) or by Lineweaver-Burk analysis which also assumes Michaelis-Menten kinetics (Figure 2a inset). The resulting parameters (V_m and $K_{m(app)}$ for 3MG uptake) are shown as mean ± SD of the analysis. The fit statistics (standard error of regression (Sy.X) and R^2) are also shown.

Table 2

[1]Inhibition of GLUT1-, GLUT3- and GLUT4-mediated 2DG uptake in HEK293 cells by quercetin, EGCG and ECG

[2]Inhibitor	[3]UTF	[4]GLUT1	[5]GLUT3	[6]GLUT4	[7]RBC-GLUT1
Quercetin					
IC_{50} (μM)	9.59 ± 1.42	2.00 ± 0.99	17.68 ± 1.71	1.70 ± 0.25	1.88 ± 0.33
$Const_1$ (M^{-1})	[8]N/A	(4.69 ± 1.92) x 10^{-5}	0.47 ± 0.02	(7.59 ± 3.75) x 10^{-8}	(4.69 ± 1.92) x 10^{-5}
$Const_2$	N/A	(2.59 ± 0.05) x 10^{4}	(5.96 ± 0. 55) x 10^{-8}	(5.95 ± 6.12) x 10^{-5}	(2.59 ± 0.05) x 10^{4}
$Const_3$ (M^{-1})	N/A	(1.79 ± 0.04) x 10^{4}	(2.77 ± 0.16) x 10^{4}	(2.37 ± 0.61) x 10^{-14}	(1.79 ± 0.04) x 10^{4}
$Const_4$ (M^{-2})	N/A	(1.17 ± 0.10) x 10^{10}	(3.05 ± 0.55) x 10^{8}	507 ± 266	(1.17 ± 0.10) x 10^{10}
EGCG					
$K_{0.5}$ (μM)	5.49 ± 1.86	9.09 ± 4.99	14.44 ± 8.19	8.45 ± 5.47	9.63 ± 1.95
$Const_1$ (M^{-1})	N/A	0.12 ± 0.03	0.28 ± 0.14	0.59 ± 0.48	0.12 ± 0.03
$Const_2$	N/A	(5.02 ± 0.33) x 10^{4}	(9.33 ± 0.53) x 10^{3}	(3.99 ± 2.44) x 10^{4}	(5.02 ± 0.33) x 10^{4}
$Const_3$ (M^{-1})	N/A	(1.03 ± 0.33) x 10^{4}	6.2 ± 3.8 x 10^{-7}	(2.37 ± 0.76) x 10^{7}	(1.03 ± 0.33) x 10^{4}
$Const_4$ (M^{-2})	N/A	(8.68 ± 0.78) x 10^{9}	4.76 ± 1.30x 10^{9}	(1.98 ± 0.86) x 10^{10}	(8.68 ± 0.78) x 10^{9}
ECG					
$K_{0.5}$ (μM)	5.54 ± 1.84	22.7 ± 17.3	199.4 ± 333.4	126.2 ± 106.3	1.90 ± 0.32
$Const_1$ (M^{-1})	N/A	(5.24 ± 2.18) x 10^{-5}	(8.37 ± 2.33) x 10^{-2}	(4.39 ± 0.87) x 10^{-2}	(5.24 ± 2.18) x 10^{-5}
$Const_2$	N/A	(4.61± 0.17) x 10^{4}	(9.38 ± 0.18) x 10^{4}	(7.94 ± 0.85) x 10^{3}	(4.61± 0.17) x 10^{4}
$Const_3$ (M^{-1})	N/A	(4.14 ± 0.17) x 10^{4}	(4.63 ± 0.12) x 10^{4}	(6.14 ± 0.89) x 10^{3}	(4.14 ± 0.17) x 10^{4}
$Const_4$ (M^{-2})	N/A	(2.48 ± 0.29) x 10^{9}	(9.54 ± 0.65) x 10^{8}	(1.06 ± 0.38) x 10^{8}	(1.84 ± 0.29) x 10^{10}

[1]The data of Figures 3 (3MG uptake at 4ºC) and 7 (2DG uptake at 37ºC) were analyzed by non-linear regression assuming that uptake inhibition is described by equation 1 (to yield IC_{50}) or by equation 3 (to yield $Const_{1\text{-}4}$). [2]Results are shown quercetin, EGCG and ECG-modulations of sugar transport. Assuming equation 3 describes intramolecular cis-allostery (*19*), $Const_1$ and $Const_3$ have units of M^{-1}, $Const_4$ has units of M^{-2} and $Const_2$ is dimensionless. Results are summarized for [3]untransfected cells, [4]GLUT1-transfected cells, [5]GLUT3-transfected cells, [6]GLUT4-transfected cells and, for comparison, for [7]GLUT1-expressing human RBCs. [8]Equation 3 analysis is not applicable to untransfected cells.

Figure 1

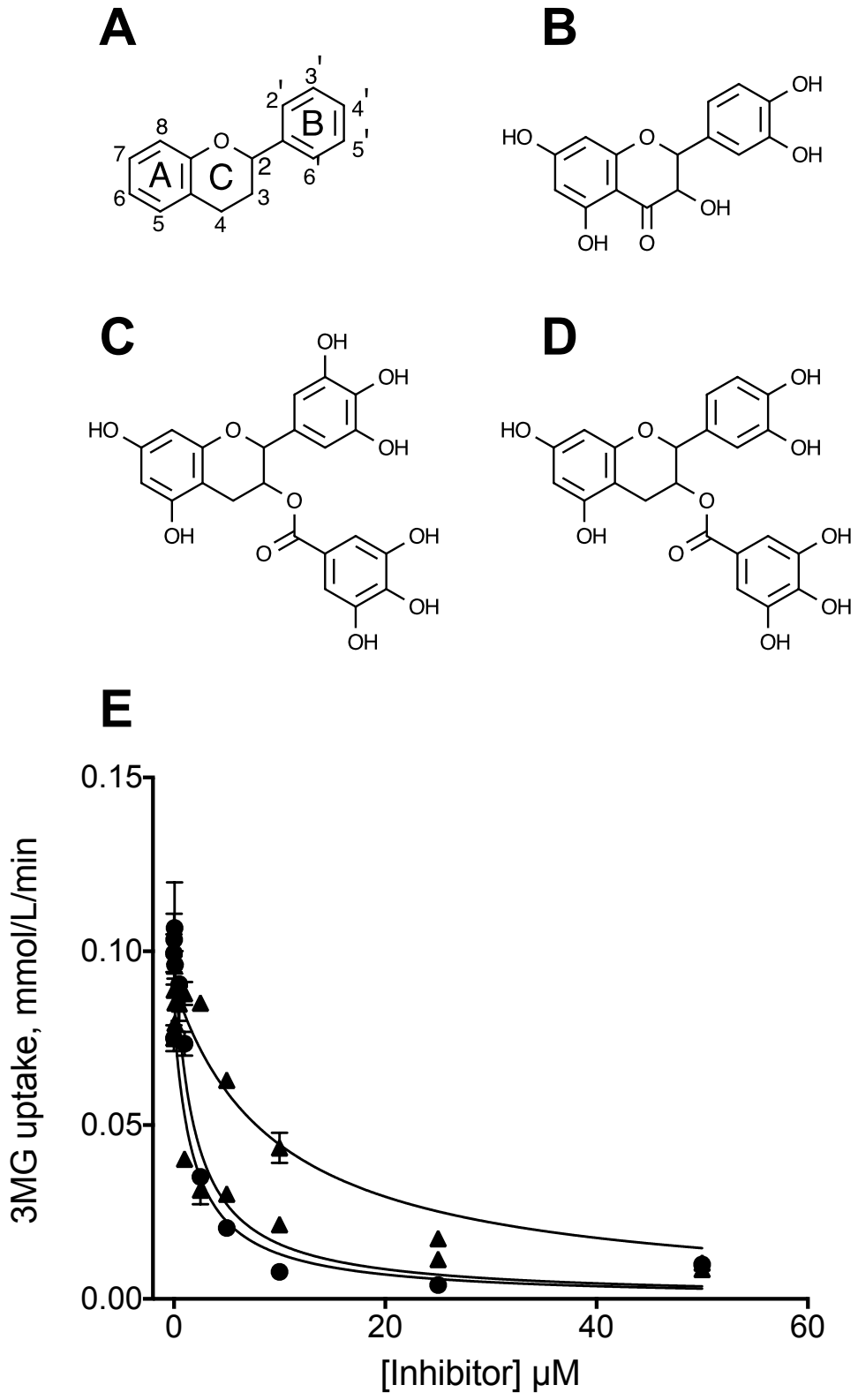

Figure 2

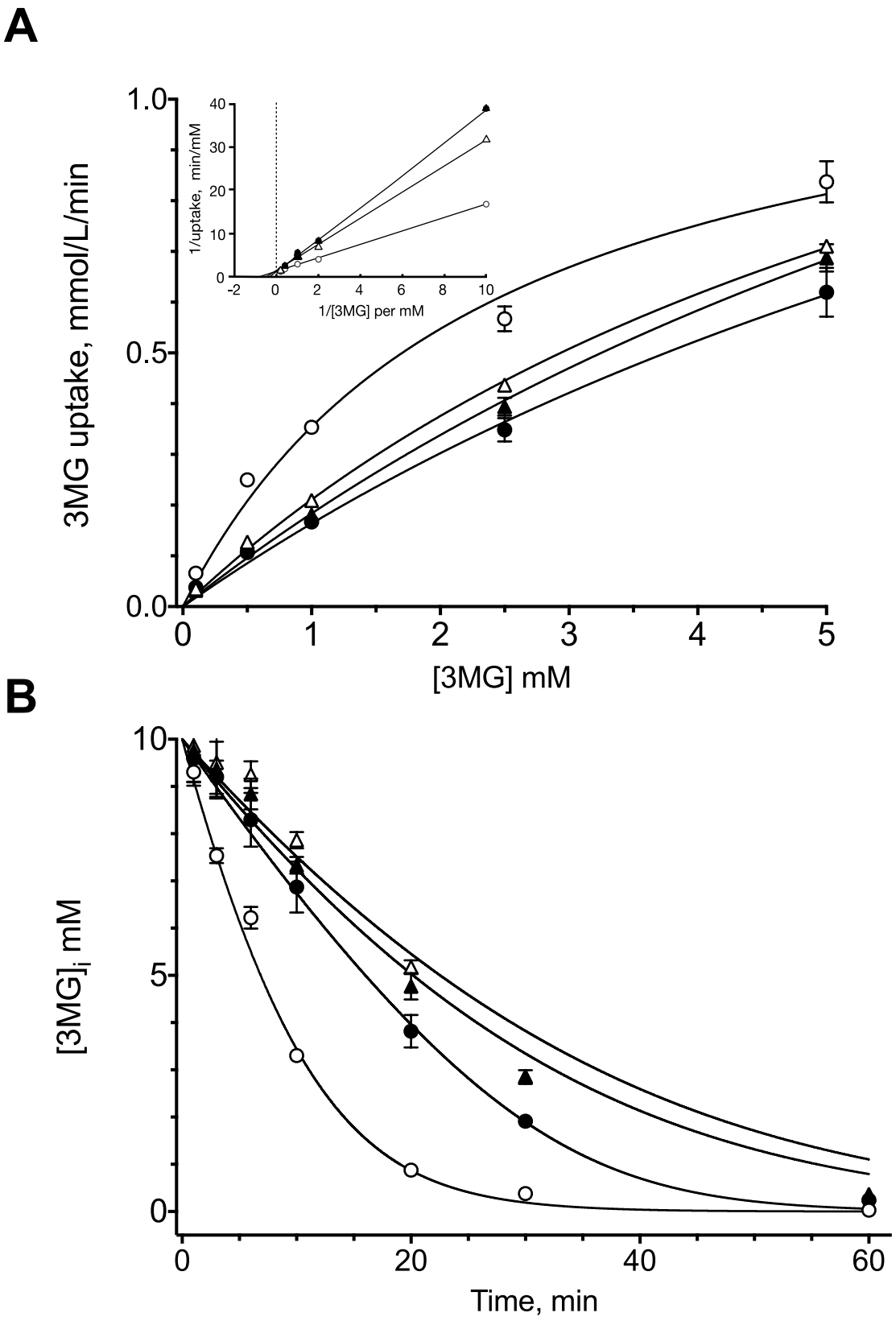

Figure 3

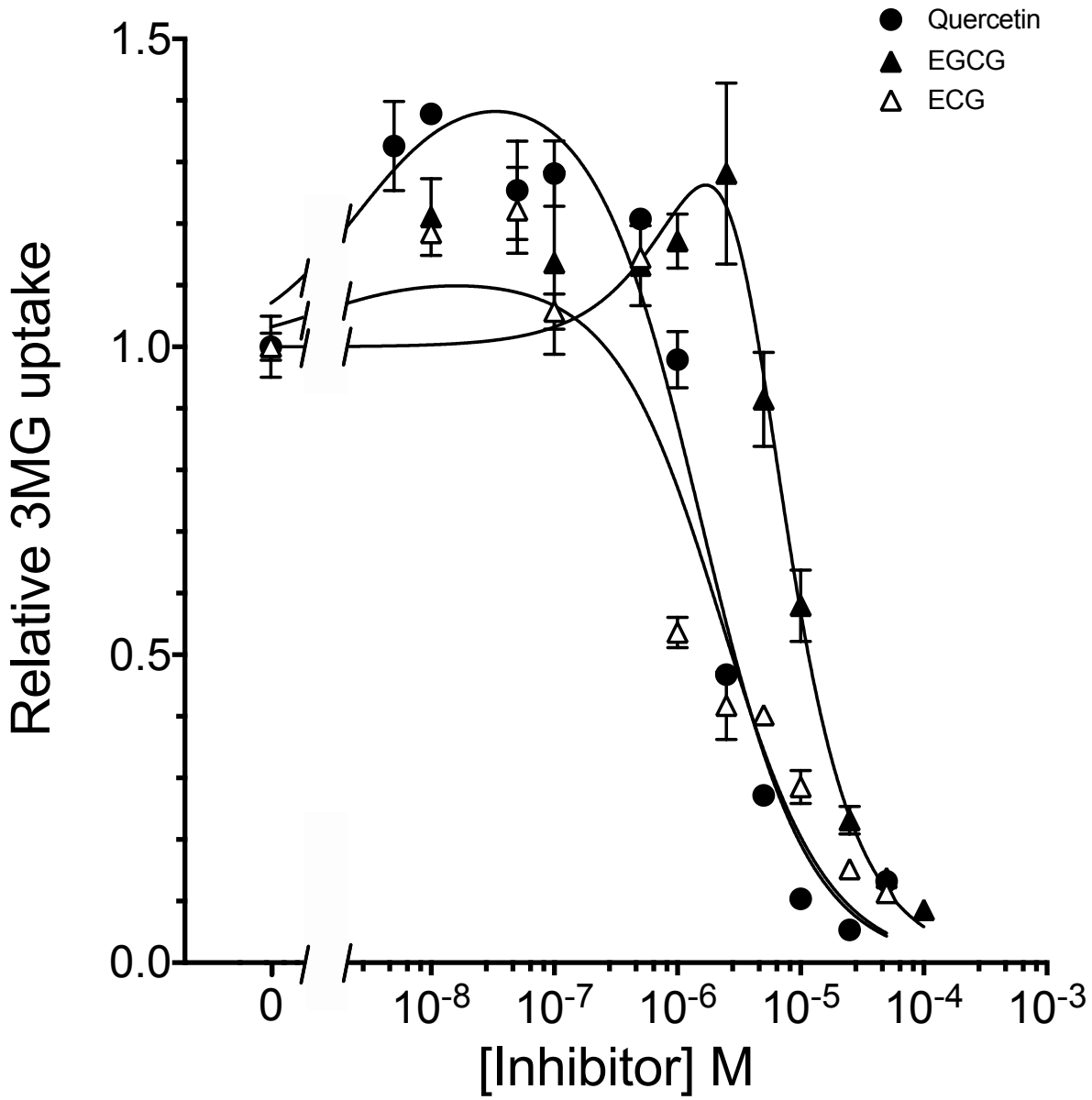

Figure 4

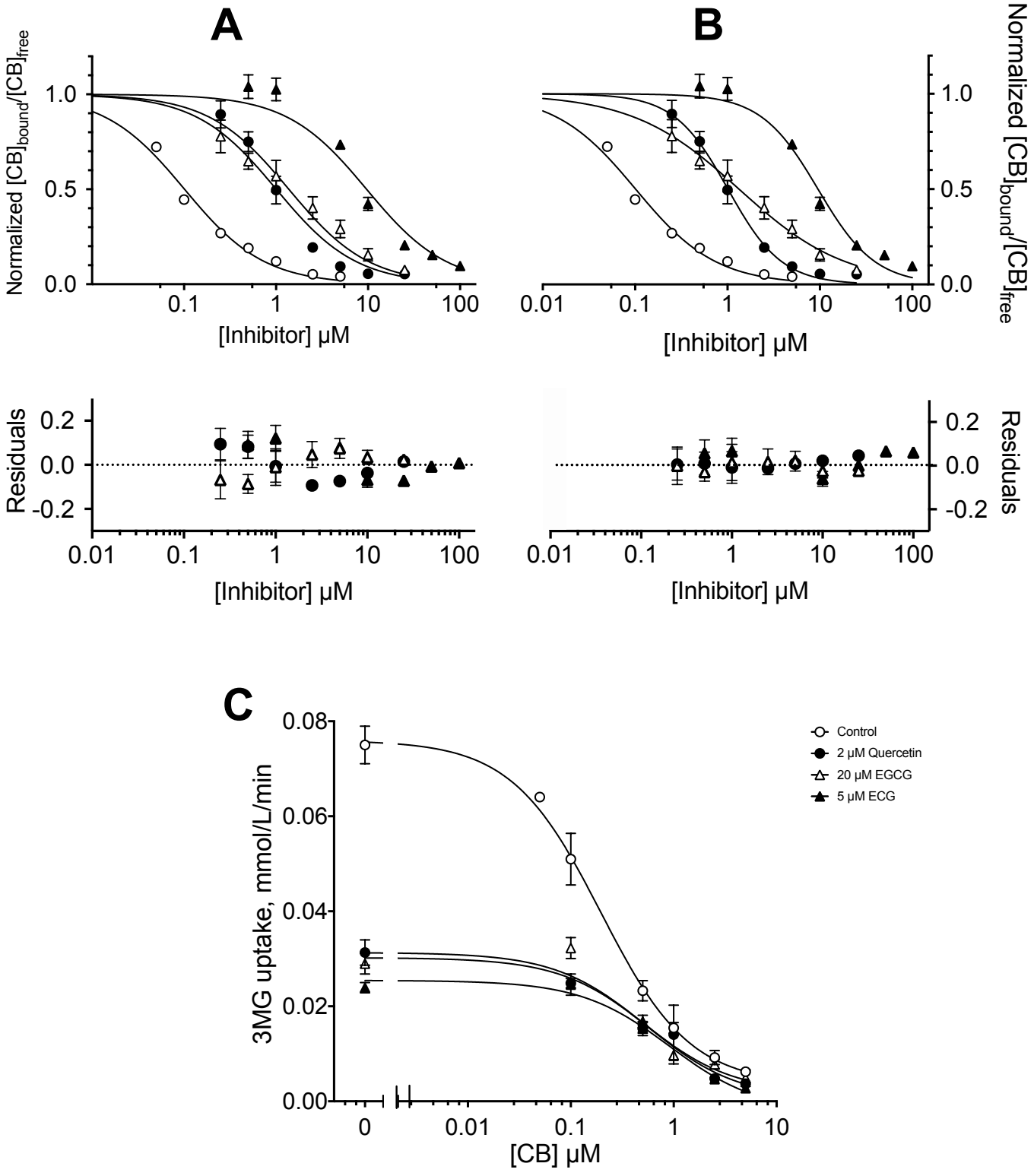

Figure 5

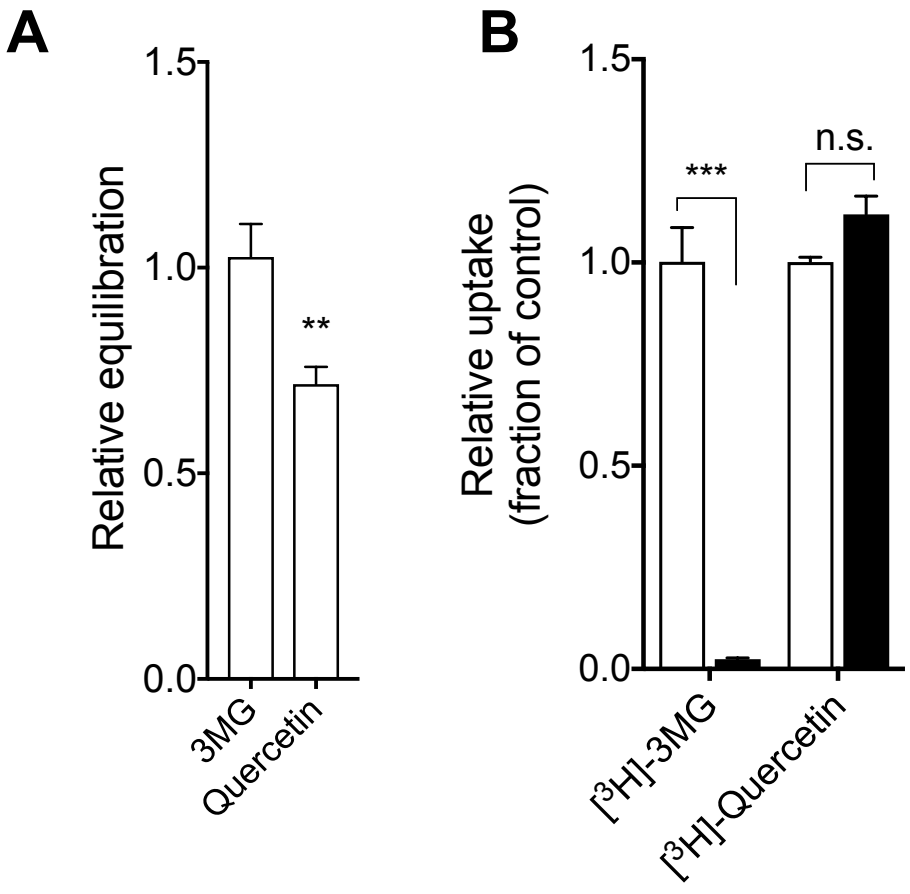

Figure 6

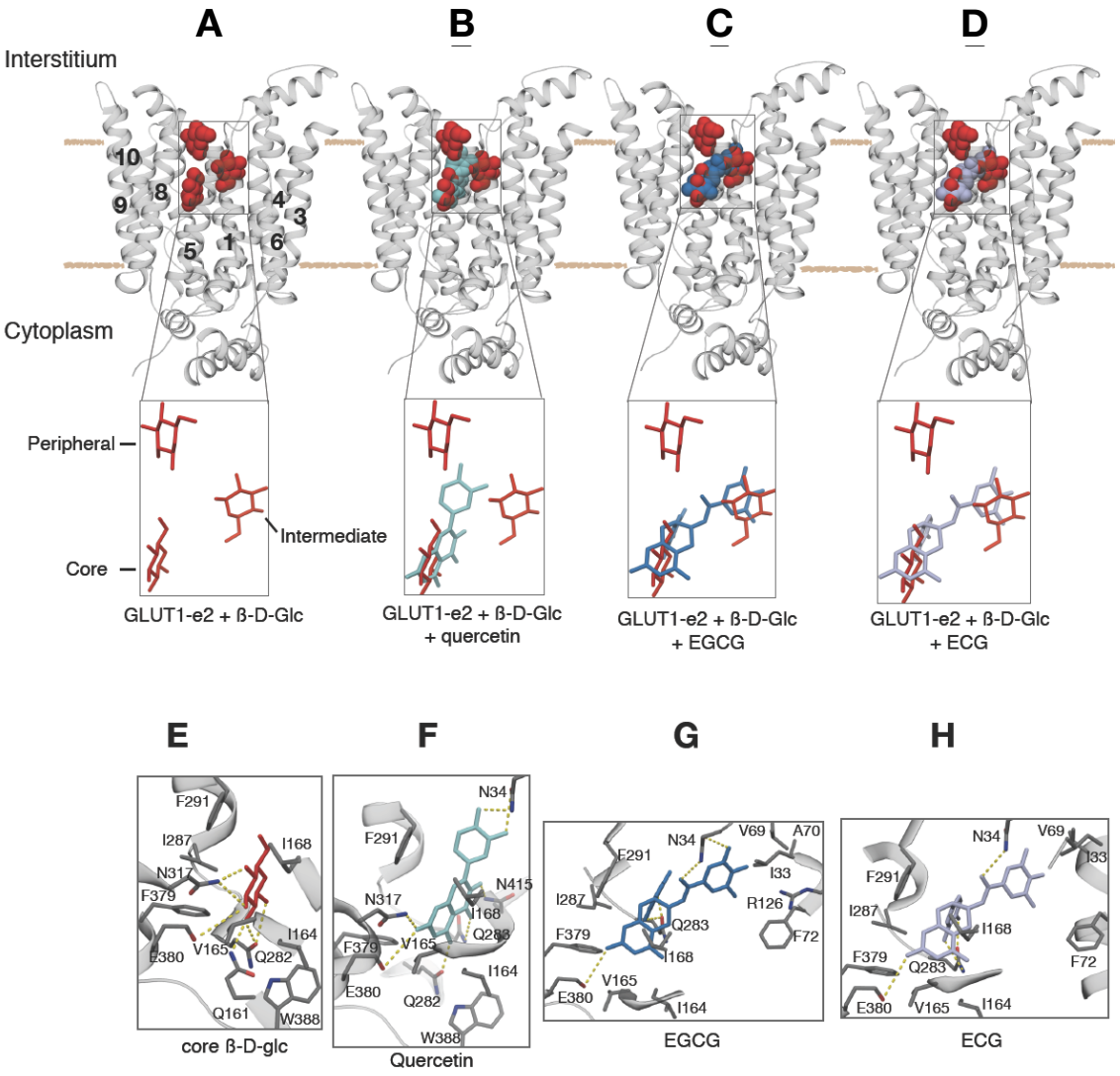

Figure 7

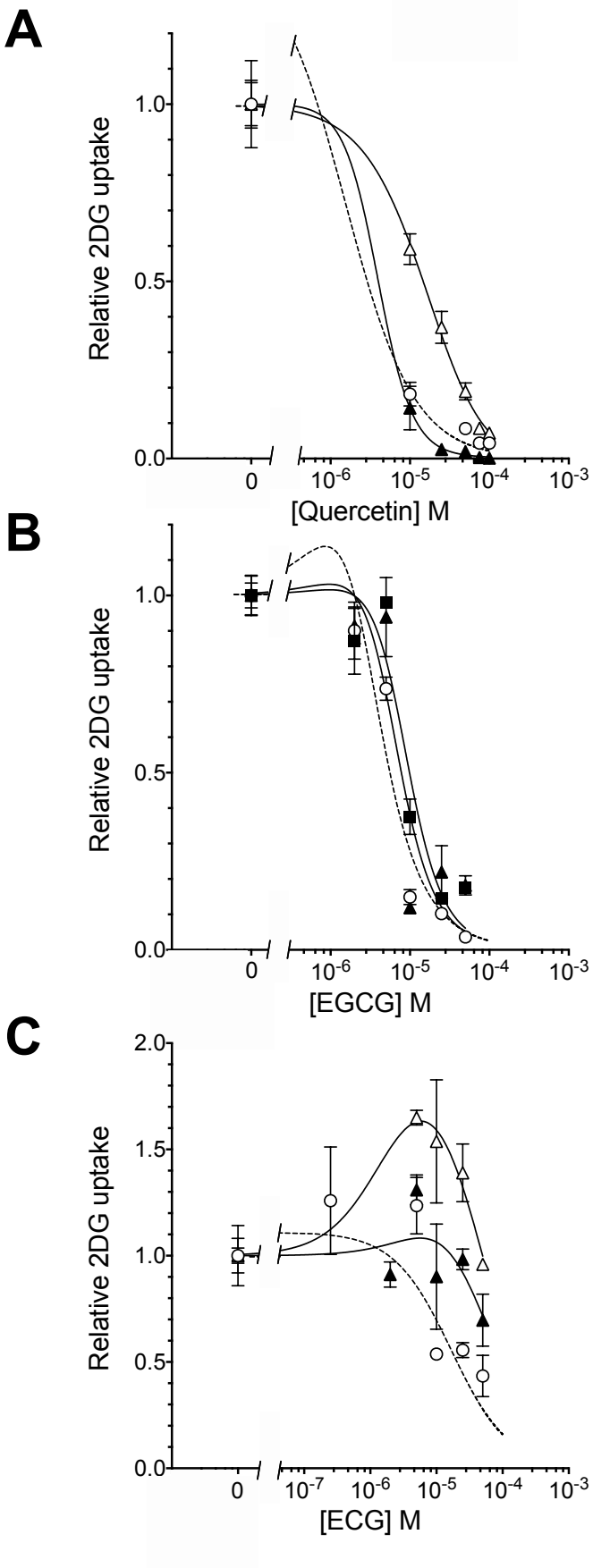

Figure 8

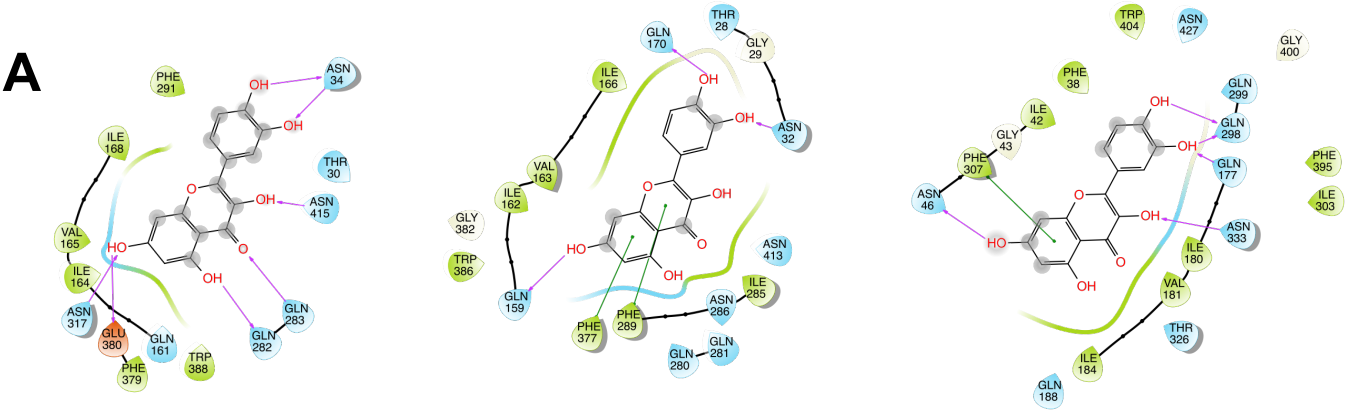

Red wine and green tea flavonoids are cis-allosteric activators and competitive inhibitors of GLUT1-mediated sugar uptake

Ogooluwa A Ojelabi, Kenneth P Lloyd, Julie K De Zutter and Anthony Carruthers

J. Biol. Chem. published online October 25, 2018
